7-14 Ward† studied the chemisorption of hydrogen on small copper particles at 25°C. His data for one run are:

Hydrogen pressure cm of Hg	Vol. of hydrogen adsorbed, cm^3 at 25°C and 1 atm
0.019	0.042
0.066	0.138
0.097	0.163
0.101	0.161
0.110	0.171
0.190	0.221
0.265	0.256
0.405	0.321
0.555	0.371
0.750	0.411
0.815	0.421
1.19	0.471
1.75	0.550

Do these data fit the Langmuir isotherm or the Freundlich isotherm?

† A. F. H. Ward, *Proc. Roy. Soc.* (*London*), **A133**, 506 (1931).

CHAPTER

EIGHT

SOLID CATALYSTS

In Chap. 7 general concepts of catalysis were discussed. Now we want to examine solid catalysts specifically. Such catalysts depend for their activity in part, at least, on the extent of surface area. It is difficult to obtain outer surface areas of more than 1 m^2/g by subdividing nonporous solids into small particles (see Example 8-1). To be effective, most catalytic solids must have surface areas in the 5 to 1000 m^2/g range. Hence, solid catalysts are normally porous. For such materials the geometrical properties of the pores can affect the global reaction rate. The objective of the first part of this chapter is to present methods of measuring the pertinent physical (geometric) properties. Following this is a discussion of theories of the catalytic behavior of solids along with a listing of typical catalysts for various types of reactions. Finally, practical aspects, such as catalyst preparation, poisons, and parameters, are treated.

The importance of surface area for catalytic activity is immediately evident by considering nickel. This metal is an active catalyst under certain conditions for oxidation and hydrogenation because it absorbs oxygen and hydrogen. The surface area of a solid has a pronounced effect on the amount of gas adsorbed and on its activity as a catalyst. For example, if a sample of fresh Raney nickel, which is highly porous and has a large surface, is held in the hand, the heat due to adsorption of oxygen can be felt immediately. No evidence of heat is apparent when a single piece of nonporous nickel of the same mass is held. This relationship between surface area and extent of adsorption has led to the development of highly porous materials with areas as high as 1500 m^2/g. Sometimes the catalytic material itself can be prepared in a form with large surface area. When this is not possible, materials which can be so prepared may be used as a *carrier* or *support* on which the catalytic substance is dispersed. Silica gel and alumina are widely used as supports.

The dependence of rates of adsorption and catalytic reactions on surface makes it imperative to have a reliable method of measuring surface area. For surface areas in the range of hundreds of square meters per gram a porous material with equivalent cylindrical pore radii (see Sec. 8-1) in the range of 10 to 100 Å is needed. The following example shows that such areas are not possible with nonporous particles of the size which can be economically manufactured.

Example 8-1 Spray drying and other procedures for manufacturing small particles can produce particles as small as 2 to 5 microns. Calculate the external surface area of nonporous spherical particles of 2 microns diameter. What size particles would be necessary if the external surface is to be 100 m^2/g (10^5 m^2/kg)? The density of the particles is 2.0 g/cm^3 (2.0×10^3 kg/m^3).

SOLUTION The external surface area per unit volume of a spherical particle of diameter d_p is

$$\frac{\pi d_p^2}{\pi d_p^3/6} = \frac{6}{d_p}$$

If the particle density is ρ_p, the surface area, per gram of particles, would be

$$S_g = \frac{6}{\rho_p d_p}$$

For $d_p = 2$ microns (2×10^{-4} cm) and $\rho_p = 2.0$ g/cm^3

$$S_g = \frac{6}{2(2 \times 10^{-4})} = 1.5 \times 10^4 \text{ cm}^2/\text{g } (1.5 \times 10^3 \text{ m}^2/\text{kg})$$

or

$$S_g = 1.5 \text{ m}^2/\text{g } (1.5 \times 10^3 \text{ m}^2/\text{kg})$$

This is about the largest surface area to be expected for nonporous particles. If a surface of 100 m^2/g were required, the spherical particles would have a diameter of

$$d_p = \frac{6}{\rho_p S_g} = \frac{6}{2.0(100 \times 10^4)} = 0.03 \times 10^{-4} \text{ cm } (0.03 \times 10^{-6} \text{ m})$$

or

$$d_p = 0.03 \text{ micron}$$

Particles as small as this cannot, at present, be produced economically. It may be noted that the smaller particles found in a fluidized-bed reactor are retained on 400 mesh screen, which has a sieve opening of 37 microns.

The quantitative effects of intraparticle mass and energy transfer on the rate when a reaction occurs on the interior pore surface of a catalyst particle is treated in Chap. 11. The method of predicting their effects requires a geometric model for the extent and distribution of void spaces within the complex porous structure of the particle. It would be best to know the size and shape of each void space in the particle. In the absence of this information the parameters in the model should be evaluated from reliable and readily obtainable average properties. In addition to the surface area, three other properties fall into this classification: void volume, the density of the solid material in the particle, and the distribution of void volume according to void size (pore-volume distribution). The methods of measurement of these four properties are considered in Secs. 8-1 to 8-3.

8-1 Determination of Surface Area

The standard method for measuring catalyst areas is based on the physical adsorption of a gas on the solid surface. Usually the amount of nitrogen adsorbed at equilibrium at the normal boiling point (−195.8°C) is measured over a range of nitrogen pressures below 1 atm. Under these conditions several layers of molecules may be adsorbed on top of each other on the surface. The amount adsorbed when one molecular layer is attained must be identified in order to determine the area. The historical steps in the development of the Brunauer-Emmett-Teller method† are clearly explained by Emmett.‡ There may be some uncertainty as to whether the values given by this method correspond exactly to the surface area. However, this is relatively unimportant, since the procedure is standardized and the results are reproducible. It should be noted that the surface area so measured may not be the area effective for catalysis. Only certain parts of the surface, the active centers, may be active for chemisorption of a reactant, while nitrogen may be physically adsorbed on much more of the surface. When the catalyst is dispersed on a large-area support, only part of the support area may be covered by catalytically active atoms and this area may be several atoms in depth. Thus, the active atoms may be together in clusters so that the catalytic surface is less than if the atoms were more completely dispersed or separated. For example a nickel-on-kieselguhr catalyst was found to have a surface of 205 m^2/g as measured by nitrogen adsorption.§ To determine the area covered by nickel atoms, hydrogen was chemisorbed on the catalyst at 25°C. From the amount of hydrogen chemisorbed, the surface area of nickel atoms was calculated to be about 40 m^2/g. It would be useful to know surface areas for chemisorption of the reactant at reaction conditions. However, this would require measurement of relatively small amounts of chemisorption at different, and often troublesome, conditions (high temperature and/or pressure), for each reaction system. In contrast, nitrogen can be adsorbed easily and rapidly in a routine fashion with standard equipment.

In the classical method of determining surface area an all-glass apparatus is used to measure the volume of gas adsorbed on a sample of the solid material.¶

† S. Brunauer, P. H. Emmett, and E. Teller, *J. Am. Chem. Soc.*, **60**, 309 (1938).

‡ P. H. Emmett (ed.), "Catalysis," vol. I, chap. 2. Reinhold Publishing Corporation, New York, 1954.

§ G. Padberg and J. M. Smith, *J. Catalysis*, **12**, 111 (1968).

¶ For a complete description of apparatus and techniques see L. G. Joyner, "Scientific and Industrial Glass Blowing and Laboratory Techniques," Instruments Publishing Company, Pittsburgh, 1949; see also S. Brunauer, "The Adsorption of Gases and Vapors," vol. I, Princeton University Press, Princeton, N.J., 1943.

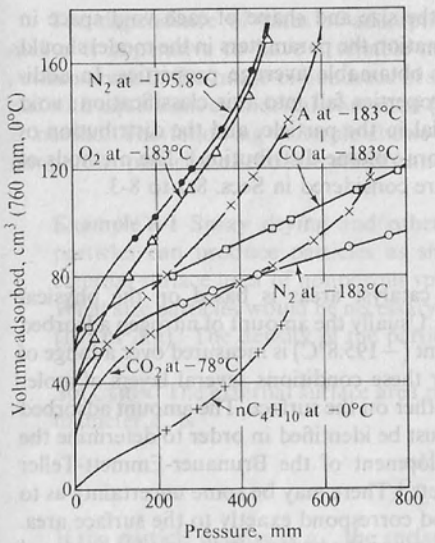

Figure 8-1 Adsorption isotherms for various gases on a 0.606-g sample of silica gel [*by permission from P. H. Emmett (ed.), "Catalysis," vol. I, Reinhold Publishing Corporation, New York, 1954*].

The apparatus operates at a low pressure which can be varied from near zero up to about 1 atm. The operating temperature is in the range of the normal boiling point. The data obtained are gas volumes at a series of pressures in the adsorption chamber. The observed volumes are normally corrected to cubic centimeters at 0°C and 1 atm (standard temperature and pressure) and plotted against the pressure in millimeters, or as the ratio of the pressure to the vapor pressure at the operating temperature. Typical results from Brunauer and Emmett's work† are shown in Fig. 8-1 for the adsorption of several gases on a 0.606-g sample of silica gel. To simplify the classical experimental procedure a flow method has been developed in which a mixture of helium (or other nonadsorbed gas) and the gas to be adsorbed is passed continuously over the sample of solid.‡ The operating total pressure is constant, and the partial pressure of adsorbable gas is varied by changing the composition of the mixture. The procedure§ is to pass a mixture of known composition over the sample until equilibrium is reached, that is, until the solid has adsorbed an amount of adsorbable component corresponding to equilibrium at its partial pressure in the mixture. Then the gas is desorbed by heating the sample while a stream of pure helium flows over it. The amount desorbed is measured with a thermal-conductivity cell or other detector. This gives one point on an isotherm, such as shown in Fig. 8-1. Then the process is repeated at successively different compositions of the mixture until the whole isotherm is obtained.

† S. Brunauer and P. H. Emmett, *J. Am. Chem. Soc.*, **59**, 2682 (1937).

‡ F. M. Nelson and F. T. Eggertsen, *Anal. Chem.*, **30**, 1387 (1958).

§ A description of the operating procedure and the data obtained are given by S. Masamune and J. M. Smith [*AIChE J.*, **10**, 246 (1964)] for the adsorption of nitrogen on Vycor (porous glass).

The curves in Fig. 8-1 are similar to the extent that at low pressures they rise more or less steeply and then flatten out for a linear section at intermediate pressures. After careful analysis of much data it was concluded that the lower part of the linear region corresponded to complete monomolecular adsorption. If this point could be located with precision, the volume of one monomolecular layer of gas, v_m, could then be read from the curve and the surface area evaluated. The Brunauer-Emmett-Teller method locates this point from an equation obtained by extending the Langmuir isotherm to apply to multilayer adsorption. The development is briefly summarized as follows: Equation (7-12) can be rearranged to the form

$$\frac{p}{v} = \frac{1}{Kv_m} + \frac{p}{v_m} \tag{8-1}$$

Brunauer, Emmett, and Teller adapted this equation for multilayer adsorption and arrived at the result

$$\frac{p}{v(p_0 - p)} = \frac{1}{v_m c} + \frac{(c-1)p}{cv_m p_0} \tag{8-2}$$

where p_0 is the saturation or vapor pressure and c is a constant for the particular temperature and gas-solid system.

According to Eq. (8-2), a plot of $p/v(p_0 - p)$ vs. p/p_0 should give a straight line. The data of Fig. 8-1 are replotted in this fashion in Fig. 8-2. Of additional significance is the fact that such straight lines can be accurately extrapolated to

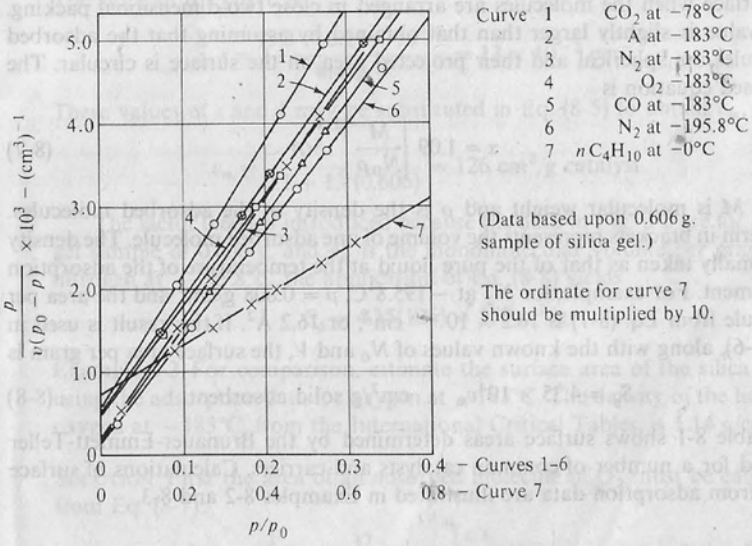

Figure 8-2 Plot of Brunauer-Emmett-Teller equation [Eq. (8-2)] for data of Fig. 8-1 [*by permission from P. H. Emmett (ed.), "Catalysis," vol. I, Reinhold Publishing Corporation, New York, 1954*].

$p/p_0 = 0$. The intercept I obtained from this extrapolation, along with the slope s of the straight line, gives two equations from which v_m can be obtained,

$$I = \frac{1}{v_m c} \qquad \text{at } p/p_0 = 0 \tag{8-3}$$

$$s = \frac{c - 1}{v_m c} \tag{8-4}$$

Solving these equations for the volume of adsorbed gas corresponding to a monomolecular layer gives

$$v_m = \frac{1}{I + s} \tag{8-5}$$

The volume v_m can be readily converted to the number of molecules adsorbed. However, to determine the surface area it is necessary to select a value for the area covered by one adsorbed molecule. If this is α, the total surface area is given by

$$S_g = \left[\frac{v_m N_0}{V}\right]\alpha \tag{8-6}$$

where N_0 is Avogadro's number, 6.02×10^{23} molecules/mol, and V is the volume per mole of gas at conditions of v_m. Since v_m is recorded at standard temperature and pressure, $V = 22{,}400$ cm^3/g mol. The term in brackets represents the number of molecules adsorbed. If v_m is based on a 1.0 g sample, then S_g is the total surface per gram of solid adsorbent.

Emmett and Brunauer† proposed that α is the projected area of a molecule on the surface when the molecules are arranged in close two-dimensional packing. This value is slightly larger than that obtained by assuming that the adsorbed molecules are spherical and their projected area on the surface is circular. The proposed equation is

$$\alpha = 1.09\left[\frac{M}{N_0 \rho}\right]^{2/3} \tag{8-7}$$

where M is molecular weight and ρ is the density of the adsorbed molecules. The term in brackets represents the volume of one adsorbed molecule. The density is normally taken as that of the pure liquid at the temperature of the adsorption experiment. For example, for N_2 at -195.8°C, $\rho = 0.808$ g/cm^3 and the area per molecule from Eq. (8-7) is 16.2×10^{-16} cm^2, or 16.2 Å^2. If this result is used in Eq. (8-6), along with the known values of N_0 and V, the surface area per gram is

$$S_g = 4.35 \times 10^4 v_m \qquad \text{cm}^2\text{/g solid adsorbent} \tag{8-8}$$

Table 8-1 shows surface areas determined by the Brunauer-Emmett-Teller method for a number of common catalysts and carriers. Calculations of surface areas from adsorption data are illustrated in Examples 8-2 and 8-3.

† P. H. Emmett and S. Brunauer, *J. Am. Chem. Soc.*, **59**, 1553 (1937).

Table 8-1 Surface area, pore volume, and mean pore radii for typical solid catalysts

Catalyst	Surface area, m^2/g	Pure volume, cm^3/g	Mean pore radius, Å
Activated carbons	500–1,500	0.6–0.8	10–20
Silica gels	200–600	0.4	15–100
SiO-Al_2O_3 cracking catalysts	200–500	0.2–0.7	33–150
Activated clays	150–225	0.4–0.52	100
Activated alumina	175	0.39	45
Celite (Kieselguhr)	4.2	1.1	11,000
Synthetic ammonia catalysts, Fe	.....	0.12	200–1,000
Pumice	0.38		
Fused copper	0.23		

Source: In part from A. Wheeler, "Advances in Catalysis," vol. III, pp. 250–326, Academic Press, Inc., New York, 1950.

Example 8-2 From the Brunauer-Emmett-Teller plot in Fig. 8-2 estimate the surface area per gram of the silica gel. Use the data for adsorption of nitrogen at -195.8°C.

SOLUTION From curve 6 of Fig. 8-2, the intercept on the ordinate is

$$I = 0.1 \times 10^{-3} \text{ cm}^{-3}$$

The slope of the curve is

$$s = \frac{(5.3 - 0.1) \times 10^{-3}}{0.4 - 0} = 13 \times 10^{-3} \text{ cm}^{-3}$$

These values of s and I may be substituted in Eq. (8-5) to obtain v_m,

$$v_m = \frac{10^3}{0.1 + 13\ (0.606)}\ \frac{1}{} = 126 \text{ cm}^3\text{/g catalyst}$$

The factor 0.606 is introduced because the data in Fig. 8-2 are for a silica gel sample of 0.606 g, and v_m is the monomolecular volume per gram. For nitrogen at -195.8°C, the application of Eq. (8-8) yields

$$S_g = 4.35(126) = 550 \text{ m}^2\text{/g}$$

Example 8-3 For comparison, estimate the surface area of the silica gel by using the adsorption data for oxygen at -183°C. The density of the liquefied oxygen at -183°C, from the International Critical Tables, is 1.14 g/cm.

SOLUTION First the area of an adsorbed molecule of O_2 must be calculated from Eq. (8-7):

$$\alpha = 1.09\left[\frac{32}{(6.02 \times 10^{23})1.14}\right]^{2/3} = 14.2 \times 10^{-16} \text{ cm}^2$$

With this value of α Eq. (8-6) gives

$$S_g = \frac{v_m(6.02 \times 10^{23})}{22{,}400} 14.2 \times 10^{-16} = 3.8 \times 10^4 v_m \qquad \text{cm}^2/\text{g}$$

From curve 4 of Fig. (8-2),

$$I = 0.40 \times 10^{-3} \text{ cm}^{-3}$$

$$s = \frac{(5.4 - 0.4) \times 10^{-3}}{0.38 - 0} = 13.2 \times 10^{-3} \text{ cm}^{-3}$$

Then the monomolecular volume per gram of silica gel is, from Eq. (8-5),

$$v_m = \frac{10^3}{0.4 + 13.2} \frac{1}{(0.606)} = 122 \text{ cm}^3/\text{g catalyst}$$

Finally, substituting this value of v_m in the area expression gives

$$S_g = 3.8 \times 10^4(122) = 465 \times 10^4 \text{ cm}^2/\text{g} \qquad \text{or } 465 \text{ m}^2/\text{g}$$

The difference in area determined from the N_2 and O_2 data is somewhat larger than expected for these gases. The adsorption curve for N_2 at $-183°C$ gives a value in closer agreement with 550 m^2/g (see Prob. 8-4).

8-2 Void Volume and Solid Density

The void volume, or pore volume, of a catalyst particle can be estimated by boiling a weighed sample immersed in a liquid such as water. After the air in the pores has been displaced, the sample is superficially dried and weighed. The increase in weight divided by the density of the liquid gives the pore volume.

A more accurate procedure is the *helium-mercury method*. The volume of helium displaced by a sample of catalyst is measured; then the helium is removed, and the volume of mercury that is displaced is measured. Since mercury will not fill the pores of most catalysts at atmospheric pressure, the difference in volumes gives the pore volume of the catalyst sample. The volume of helium displaced is a measure of the volume occupied by the solid material. From this and the weight of the sample, the density of the solid phase, ρ_S, can be obtained. Then the void fraction, or porosity, of the particle, ε_p, may be calculated from the equation

$$\varepsilon_p = \frac{\text{void (pore) volume of particle}}{\text{total volume of particle}} = \frac{m_p V_g}{m_p V_g + m_p(1/\rho_S)}$$

$$= \frac{V_g \rho_S}{V_g \rho_S + 1} \tag{8-9}$$

where m_p is the mass of the particle and V_g is the void volume per gram of particles. If the sample of particles is weighed, the mass divided by the mercury volume gives the density ρ_p of the porous particles. Note that the porosity is also obtainable from this density by the expression

$$\varepsilon_p = \frac{\text{void volume}}{\text{total volume}} = \frac{V_g}{1/\rho_p} = \rho_p V_g \tag{8-10}$$

From the helium-mercury measurements the pore volume, the solid density, and the porosity of the catalyst particle can be determined. Values of ε_p are of the order of 0.5, indicating that the particle is about half void space and half solid material. Since overall void fractions in packed beds are about 0.4, a rule of thumb for a packed-bed catalytic reactor is that about 30% of the volume is pore space, 30% is solid catalyst and carrier, and 40% is void space between catalyst particles. Individual catalysts may show results considerably different from these average values, as indicated in Examples 8-4 and 8-5 and Table 8-2.

Example 8-4 In an experiment to determine the pore volume and catalyst-particle porosity the following data were obtained on a sample of activated silica (granular, 4 to 12 mesh size):

- Mass of catalyst sample placed in chamber = 101.5 g
- Volume of helium displaced by sample = 45.1 cm^3
- Volume of mercury displaced by sample = 82.7 cm^3

Calculate the required properties.

SOLUTION The volume of mercury displaced, minus the helium-displacement volume, is the pore volume. Hence

$$V_g = \frac{82.7 - 45.1}{101.5} = 0.371 \text{ cm}^3/\text{g}$$

The helium volume is also a measure of the density of the solid material in the catalyst; that is,

$$\rho_S = \frac{101.5}{45.1} = 2.25 \text{ g/cm}^3$$

Substituting the values of V_g and ρ_S in Eq. (8-9) gives the porosity of the silica gel particles,

$$\varepsilon_p = \frac{0.371(2.25)}{0.371(2.25) + 1} = 0.455$$

Catalyst particles used in packed-bed reactors normally are pelleted, or agglomerated by other means, to sizes of $\frac{1}{16}$ in. to $\frac{1}{2}$ in. in order to avoid excessive pressure drop and to provide mechanical strength. Usually the pellets are cylindrical or granular. Agglomeration of *porous* particles gives a pellet containing two void regions: small void spaces within the individual particles and larger spaces between particles. Hence such materials are said to contain *bidisperse pore systems*. Although the shape and nature of these two void regions may vary from thin cracks to a continuous region surrounding a group of particles, it has been customary to designate both regions as *pores*. The void spaces within the particles are commonly termed *micropores*, and the void regions between particles are called *macropores*. *Particle* refers only to the small individual unit from which the pellet is produced.

Perhaps the most widely used pellets are those of alumina. Porous alumina particles (20 to 200 microns diameter) containing micropores of 10 to 200 Å

Table 8-2 Physical properties of alumina pellets

Density, g/cm³		Pore volume, cm³/g		Void fraction		
Particle	Pellet	Micro	Macro	Total	Macro	Micro
1.292	1.121	0.365	0.120	0.543	0.134	0.409
1.264	1.010	0.383	0.198	0.587	0.200	0.387
1.238	0.896	0.400	0.308	0.634	0.275	0.359
1.212	0.785	0.416	0.451	0.680	0.353	0.327
1.188	0.672	0.434	0.670	0.725	0.450	0.275

Notes: All properties are based on Al_2O_3. Micro refers to pore radii less than 100 Å, and macro refers to radii greater than 100 Å.

Source: R. A. Mischke and J. M. Smith, *Ind. Eng. Chem., Fund. Quart.*, **1**, 288 (1962).

diameter are readily prepared by spray drying. These somewhat soft particles are easily made into pellets. The macroporosity and macropore diameter depend on the pelleting pressure and can be varied over a wide range. Table 8-2 shows macro and micro properties of five alumina pellets, each prepared at a different pelleting pressure. The pellet density listed in the second column is approximately proportional to the pressure used. Comparison of the least and greatest pellet density shows that the macropore volume has decreased from 0.670 to 0.120 with increased pelleting pressure, while the micropore volume has decreased only from 0.434 to 0.365.

The external surface area of even very fine particles has been shown (Example 8-1) to be small with respect to the internal surface of the pores. Hence, in a catalyst pellet the surface resides predominantly in the small pores within the particles. The external surface of the particles, and of course the external area of the pellets, is negligible.

Macro- and micropore volumes and porosities for bidisperse catalyst pellets are calculated by the same methods as used for monodisperse pore systems. Example 8-5 illustrates the procedure.

Example 8-5 A hydrogenation catalyst is prepared by soaking alumina particles (100 to 150 mesh size) in aqueous $NiNO_3$ solution. After drying and reduction, the particles contain about 7 wt % NiO. This catalyst is then made into large cylindrical pellets for rate studies. The gross measurements for one pellet are

Mass = 3.15 g
Diameter = 1.00 in.
Thickness = $\frac{1}{4}$ in.
Volume = 3.22 cm³

The Al_2O_3 particles contain micropores, and the pelleting process introduces macropores surrounding the particles. From the experimental methods already described, the macropore volume of the pellet is 0.645 cm³ and the micropore volume is 0.40 cm³/g of particles. From this information calculate:

(*a*) The density of the *pellet*
(*b*) The macropore volume in cubic centimeters per gram
(c) The macropore void fraction in the *pellet*
(*d*) The micropore void fraction in the *pellet*
(*e*) The solid fraction
(*f*) The density of the *particles*
(*g*) The density of the solid phase
(*h*) The void fraction of the *particles*

SOLUTION

(*a*) The density of the pellet is

$$\rho_P = \frac{3.15}{3.22} = 0.978 \text{ g/cm}^3$$

(*b*) The macropore volume per gram is

$$(V_g)_M = \frac{0.645}{3.15} = 0.205 \text{ cm}^3/\text{g}$$

(*c*) The macropore void fraction ε_M is obtained by applying Eq. (8-10) to the pellet. Thus

$$\varepsilon_M = \frac{\text{macropore volume}}{\text{total volume}} = \frac{(V_g)_M}{1/\rho_P} = \frac{0.205}{1/0.978} = 0.200$$

(*d*) Since

$$(V_g)_\mu = 0.40 \text{ cm}^3/\text{g}$$

the micropore void fraction ε_μ in the pellet is

$$\varepsilon_\mu = \frac{(V_g)_\mu}{1/\rho_P} = \frac{0.40}{1/0.978} = 0.391$$

(*e*) The solids fraction ε_S is given by

$$1 = \varepsilon_M + \varepsilon_\mu + \varepsilon_S$$

$$\varepsilon_S = 1 - 0.200 - 0.391 = 0.409$$

(*f*) The density ρ_p of the *particles* can be calculated by correcting the total volume of the *pellet* for the macropore volume. Thus

$$\rho_p = \frac{3.15}{3.22 - 0.645} = 1.22 \text{ g/cm}^3$$

or, in terms of 1 g of pellet,

$$\rho_p = \frac{1}{1/\rho_P - (V_g)_M} = \frac{\rho_P}{1 - (V_g)_M \rho_P}$$

$$\rho_p = \frac{0.978}{1 - 0.205(0.978)} = 1.22 \text{ g/cm}^3$$

(*g*) The density of the solid phase is

$$\rho_S = \frac{\text{mass of pellet}}{(\text{volume of pellet})\,\varepsilon_S}$$

$$= \frac{\rho_P}{\varepsilon_S} = \frac{0.978}{0.409} = 2.39 \text{ g/cm}^3$$

(*h*) The void fraction of the *particles* is given by

$$\varepsilon_p = \frac{(V_g)_\mu}{1/\rho_p} = \rho_p (V_g)_\mu$$

$$= 1.22(0.40) = 0.49$$

For this pellet a fraction equal to $\varepsilon_M + \varepsilon_\mu = 0.591$ is void and 0.409 is solid. Of the individual particles, a fraction 0.49 is void. Note that all these results were calculated from the mass and volume of the pellet and the measurements of macro- and micropore volumes.

8-3 Pore-Volume Distribution

We shall see in Chap. 11 that the effectiveness of the internal surface for catalytic reactions can depend not only on the volume of the void spaces (V_g), but also on the radius of the void regions. Therefore it is desirable to know the distribution of void volume in a catalyst according to size of the pore. This is a difficult problem because the void spaces in a given particle are nonuniform in size, shape, and length, and normally are interconnected. Further, these characteristics can change from one type of catalyst particle to another. Figure 8-3 shows electron-microscope (scanning type) photographs of porous silver particles ($S_g = 19.7$ m^2/g). The material was prepared by reducing a precipitate of silver fumarate by heating at 350°C in a stream of nitrogen. The larger darker regions probably represent void space between individual particles, and the smaller dark spaces are intraparticle voids. The light portions are solid silver. The complex and random geometry shows that it is not realistic to describe the void spaces as pores. It is anticipated that other highly porous materials such as alumina and silica would have similar continuous and complex void phases. For a material such as Vycor, with its relatively low porosity (0.3) and continuous solid phase, the concept of void spaces as pores is more reasonable.

In view of evidence such as that in Fig. 8-3, it is unlikely that detailed quantitative descriptions of the void structure of solid catalysts will become available. Therefore, to account quantitatively for the variations in rate of reaction with location within a porous catalyst particle, a simplified model of the pore structure is necessary. The model must be such that diffusion rates of reactants through the void spaces into the interior surface can be evaluated. More is said about these models in Chap. 11. It is sufficient here to note that in all the widely used models the void spaces are simulated as cylindrical pores. Hence the size of the void space is interpreted as a radius a of a cylindrical pore, and the distribution of void volume is defined in terms of this variable. However, as the example of the silver

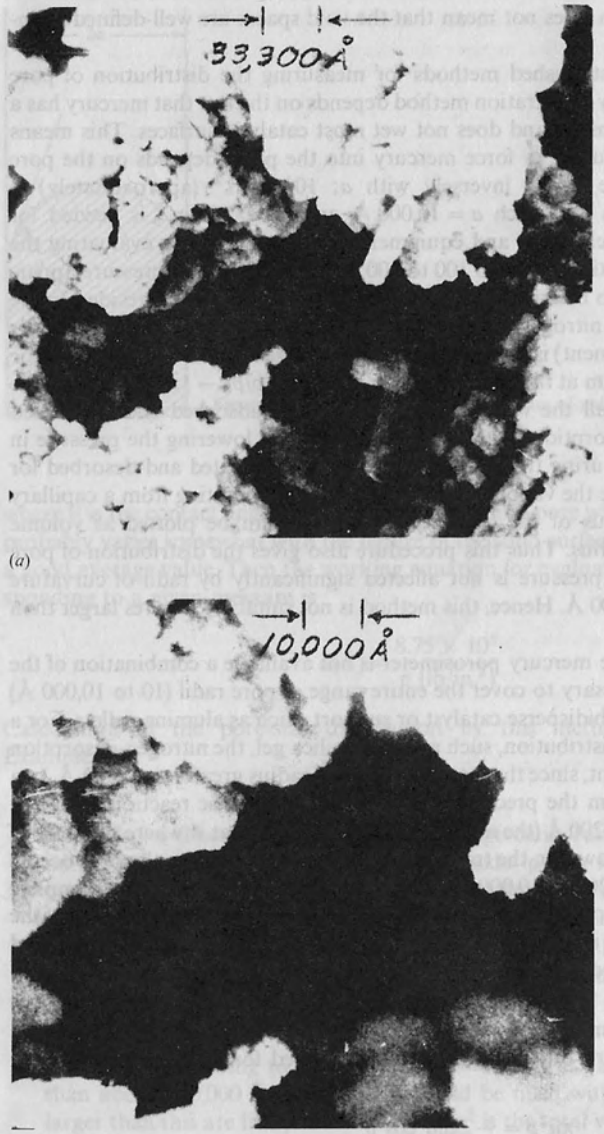

(*a*)

(*b*)

Figure 8-3 Electron micrographs of porous silver particles (approximate surface area = 19.7 m^2/g): (*a*) magnification = 3000 (1 cm = 33000 Å); (*b*) magnification = 10,000 (1 cm = 10,000 Å).

catalyst indicates, this does not mean that the void spaces are well-defined cylindrical pores.

There are two established methods for measuring the distribution of pore volumes. The mercury-penetration method depends on the fact that mercury has a significant surface tension and does not wet most catalytic surfaces. This means that the pressure required to force mercury into the pores depends on the pore radius. The pressure varies inversely with a; 100 lb/in.^{2} (approximately) is required to fill pores for which $a = 10{,}000$ Å, and 10,000 lb/in.^{2} is needed for $a = 100$ Å. Simple techniques and equipment are satisfactory for evaluating the pore-volume distribution down to 100 to 200 Å, but special high-pressure apparatus is necessary to go below $a = 100$ Å, where much of the surface resides. In the second method, the nitrogen-adsorption experiment (described in Sec. 8-1 for surface area measurement) is continued until the nitrogen pressure approaches the saturation value (1 atm at the normal boiling point). At $p/p_0 \to 1.0$, where p_0 is the saturation pressure, all the void volume is filled with adsorbed and condensed nitrogen. Then a desorption isotherm is established by lowering the pressure in increments and measuring the amount of nitrogen evaporated and desorbed for each increment. Since the vapor pressure of a liquid evaporating from a capillary depends on the radius of the capillary, these data can be plotted as volume desorbed vs. pore radius. Thus this procedure also gives the distribution of pore volumes. The vapor pressure is not affected significantly by radii of curvature greater than about 200 Å. Hence, this method is not suitable for pores larger than 200 Å.

If a high-pressure mercury porosimeter is not available a combination of the two methods is necessary to cover the entire range of pore radii (10 to 10,000 Å) which may exist in a bidisperse catalyst or support, such as alumina pellets. For a monodisperse pore distribution, such as that in silica gel, the nitrogen-desorption experiment is sufficient, since there are few pores of radius greater than 200 Å. In a bidisperse pore system the predominant part of the catalytic reaction occurs in pores less than about 200 Å (the micropore region), since that is where the bulk of the surface resides. However, the transport of reactants to these small pores occurs primarily in pores of 200 to 10,000 Å (the macropore region). Hence the complete distribution of pore volume is required in order to establish the effectiveness of the interior surface, that is, the global rate of reaction. Calculation procedures and typical results are discussed briefly in the following paragraphs.

Mercury-penetration method By equating the force due to surface tension (which tends to keep mercury out of a pore) to the applied force, Ritter and Drake† obtained

$$\pi a^2 p = -2\pi a\sigma \cos\theta$$

or

$$a = \frac{-2\sigma \cos\theta}{p} \tag{8-11}$$

† H. L. Ritter and L. C. Drake, *Ind. Eng. Chem., Anal. Ed.*, **17**, 787 (1945).

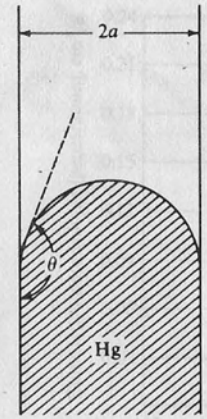

Figure 8-4 Mercury penetration in a pore of radius a.

where θ is the contact angle between the mercury and pore wall (Fig. 8-4). While θ probably varies somewhat with the nature of the solid surface, 140° appears to be a good average value. Then the working equation for evaluating the radius corresponding to a given pressure is

$$a(\text{Å}) = \frac{8.75 \times 10^5}{p\ (\text{lb/in.}^2)} \tag{8-12}$$

Calculation of the pore-size distribution by this method is illustrated in Example 8-6.

Example 8-6 The mercury-penetration data given in Table 8-3 were obtained on a 0.624-g sample of a uranium dioxide pellet formed by sintering particles at 1000°C for 2 h. Since the particles were nonporous, the void space was entirely between the particles (that is, in macropores). At the beginning of the experiment (when the pressure was 1.77 lb/in.^{2} abs) the amount of mercury displaced by the sample was found to be 0.190 cm^3. Calculate the porosity and pore-volume distribution of the pellet.

SOLUTION According to Eq. (8-12), at $p = 1.77$ lb/in.^{2} abs only pores larger than about 500,000 Å (50 microns) would be filled with mercury. No pores larger than this are likely. Hence 0.190 cm^3 is the total volume of the sample. At the highest pressure, 3,500 lb/in.^{2} abs, only pores less than $a = 250$ Å would remain unfilled. Since the pores were entirely of the macro type, few pores smaller than 250 Å are expected. Neglecting these pores, the porosity can be calculated from the porosimeter measurements alone. Thus

$$\varepsilon_p = \frac{0.125}{0.190} = 0.66$$

Table 8-3 Mercury porosimeter data for uranium dioxide pellet (mass of sample 0.624 g)

Pressure lb/in.^{2}	Mercury concentration, cm^3	Pentration, cm^3/g	
116	0.002	0.003	0.196
310	0.006	0.010	0.189
344	0.010	0.016	0.183
364	0.014	0.022	0.177
410	0.020	0.032	0.167
456	0.026	0.042	0.157
484	0.030	0.048	0.151
540	0.038	0.061	0.138
620	0.050	0.080	0.119
710	0.064	0.102	0.097
800	0.076	0.122	0.077
830	0.080	0.128	0.071
900	0.088	0.141	0.058
1,050	0.110	0.160	0.039
1,300	0.112	0.179	0.020
1,540	0.118	0.189	0.010
1,900	0.122	0.196	0.003
2,320	0.124	0.198	0.001
3,500	0.125	0.199	0

A check on this result is available from air-pycnometer† data, which gave a solid volume of 0.0565 cm^3. Thus the total porosity is

$$(\varepsilon_P)_t = \frac{0.190 - 0.0565}{0.190} = 0.70$$

The difference between values suggests that there were a few pores smaller than 250 Å in the sample, although the comparison also includes experimental errors in the two methods.

To calculate the pore-volume distribution the penetration data are first corrected to a basis of 1 g of sample, as given in the third column of Table 8-3. If we neglect the pores smaller than 250 Å, the penetration data can be reversed, starting with $V = 0$ at 3500 lb/in.^{2} abs (250 Å). The last column shows the figures. Then, from Eq. (8-12) and the pressure, the radius corresponding to each penetration value can be established. This gives the penetration curve shown in Fig. 8-5. The penetration volume at any pore radius a is the volume of pores larger than a. The derivative of this curve, $\Delta V/\Delta a$, is the volume of pores between a and $a + \Delta a$ divided by Δa; that is, it is the distribution function for the pore volume according to pore radius. It is customary to

† A device which uses air at two pressures to measure void volumes of porous materials. It provides the same data as the helium measurement described in Sec. 8-2.

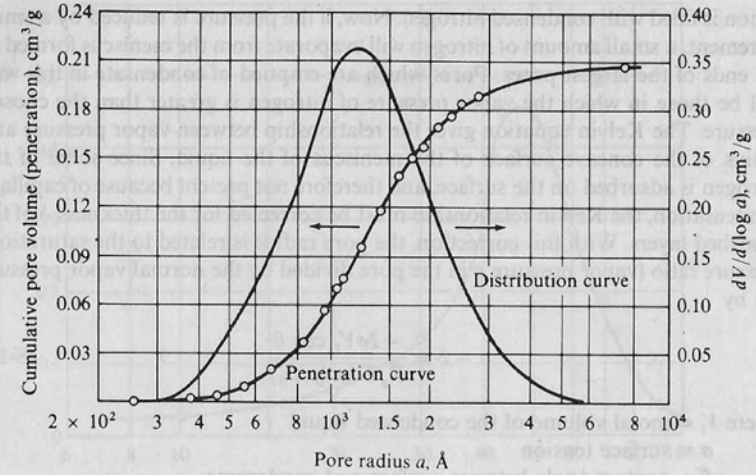

Figure 8-5 Pore-volume distribution in a UO_2 pellet.

plot the pore radius on a logarithmic coordinate as shown. Hence the distribution function is taken as the derivative of the curve so plotted, that is, dV/d (log a). The distribution function is also shown plotted against a in Fig. 8-5.

For this pellet the distribution is seen to be reasonably symmetrical with most of the volume in pores from 300 to 8000 Å and with a most probable pore radius of 1200 Å. Note that the flatness of the penetration curve at low pore radii justifies neglecting the pores smaller than 250 Å.

Wheeler† has summarized the assumptions and accuracy of the mercury-penetration method. It is important to note that erroneous results would be obtained if the porous particle contains large void spaces that are connected only to smaller void spaces. Such large "bottleneck" pores would fill with mercury at the higher pressure corresponding to the connecting smaller pores. For accurate results each porous region must be connected to at least one larger pore.

Nitrogen-desorption method As the low-temperature nitrogen-adsorption experiment (Sec. 8-1) is continued to higher pressures multilayer adsorption occurs, and ultimately the adsorbed films are thick enough to bridge the pore.‡ Then further uptake of nitrogen will result in capillary condensation. Since the vapor pressure decreases as the capillary size decreases, such condensation will occur first in the smaller pores. Condensation will be complete, as $p/p_0 \to 1.0$, when the entire void

† A. Wheeler, in P. H. Emmett (ed.), "Catalysis," vol. II, p. 123, Reinhold Publishing Corporation, New York, 1955.

‡ L. H. Cohan, *J. Am. Chem. Soc.*, **60**, 433 (1938); A. G. Foster, *J. Phys. Colloid Chem.*, **55**, 638 (1951).

region is filled with condensed nitrogen. Now, if the pressure is reduced by a small increment, a small amount of nitrogen will evaporate from the meniscus formed at the ends of the largest pores. Pores which are emptied of condensate in this way will be those in which the vapor pressure of nitrogen is greater than the chosen pressure. The Kelvin equation gives the relationship between vapor pressure and radius of the concave surface of the meniscus of the liquid. Since some of the nitrogen is adsorbed on the surface, and therefore not present because of capillary condensation, the Kelvin relationship must be corrected for the thickness δ of the adsorbed layers. With this correction, the pore radius is related to the saturation-pressure ratio (vapor pressure p in the pore divided by the normal vapor pressure p_0) by

$$a - \delta = \frac{-2\sigma V_l \cos\theta}{R_g T \ln (p/p_0)} \tag{8-13}$$

where V_l = molal volume of the condensed liquid
σ = surface tension
θ = contact angle between surface and condensate

Since nitrogen completely wets the surface covered with adsorbed nitrogen, $\theta = 0°$ and $\cos\theta = 1$. The thickness δ depends on p/p_0. The exact relationship has been the subject of considerable study.† but Wheeler's form

$$\delta(\text{Å}) = 9.52\left(\log \frac{p_0}{P}\right)^{-1/n} \tag{8-14}$$

is generally used.

For nitrogen at $-195.8°C$ (normal boiling point) Eq. (8-13), for $a - \delta$ in angstroms, becomes

$$a - \delta = 9.52\left(\log \frac{p_0}{p}\right)^{-1} \tag{8-15}$$

with δ determined from Eq. (8-14).

For a chosen value of p/p_0, Eqs. (8-15) and (8-14) give the pore radius above which all pores will be empty of capillary condensate. Hence, if the amount of desorption is measured for various p/p_0, the pore volume corresponding to various radii can be evaluated. Differentiation of the curve for cumulative pore volume vs. radius gives the distribution of volume as described in Example 8-6. Descriptions of the method of computation are given by several investigators.‡ As in the mercury-penetration method, errors will result unless each pore is connected to at least one larger pore.

Figure 8-6 shows the result of applying the method to a sample of Vycor

† A. Wheeler, in P. H. Emmett (ed.), "Catalysis," vol. II, chap. 2, Reinhold Publishing Corporation, New York, 1955; G. D. Halsey, *J. Chem. Phys.*, **16**, 931 (1948); C. G. Shull, *J. Am. Chem. Soc.*, **70**, 1405 (1948); J. O. Mingle and J. M. Smith, *Chem. Eng. Sci.*, **16**, 31 (1961).

‡ E. P. Barrett, L. G. Joyner, and P. P. Halenda, *J. Am. Chem. Soc.*, **73**, 373 (1951); C. J. Pierce, *J. Phys. Chem.*, **57**, 149 (1953); R. B. Anderson, *J. Catalysis*, **3**, 50 (1964).

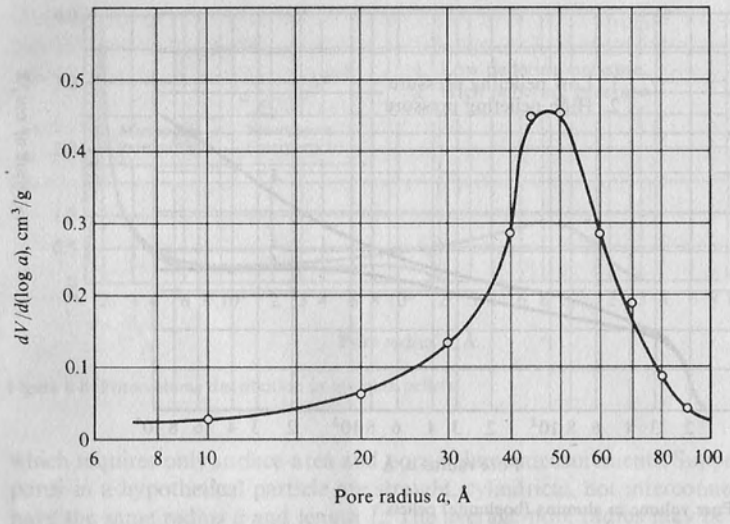

Figure 8-6 Pore-volume distribution in Vycor; $\rho_p = 1.46$ g/cm^3, $V_g = 0.208$ cm^3/g, $S_g = 90$ m^2/g.

(porous glass).† This material, which contained only micropores, had the properties

$$\rho_p = 1.46 \text{ g/cm}^3$$
$$V_g = 0.208 \text{ cm}^3/\text{g}$$
$$\varepsilon_p = 0.304$$
$$S_g = 90 \text{ m}^2/\text{g}$$

The surface area was determined from nitrogen-adsorption data in the low p/p_0 range, as described in Sec. 8-1, while the distribution results in Fig. 8-6 were established from the desorption curve in the capillary-condensation (high p/p_0) region.

By combining mercury-penetration and nitrogen-desorption measurements, pore-volume information can be obtained over the complete range of radii in a pelleted catalyst containing both macro- and micropores. Figure 8-7 shows the cumulative pore volume for two alumina pellets, each prepared by compressing porous particles of boehmite ($Al_2O_3 \cdot H_2O$). The properties‡ of the two pellets are given in Table 8-4. The only difference in the two is the pelleting pressure. Increasing this pressure causes drastic reductions in the space between particles (macropore volume) but does not greatly change the void volume within the particles or

† M. R. Rao and J. M. Smith, *AIChE J.*, **10**, 293 (1964).

‡ The properties and pore-volume distribution were determined by M. F. L. Johnson, Sinclair Research Laboratories, Harvey, Ill., by the methods described in Secs. 8-1 to 8-3. They were orginally reported in J. L. Robertson and J. M. Smith, *AIChE J.*, **9**, 344 (1963).

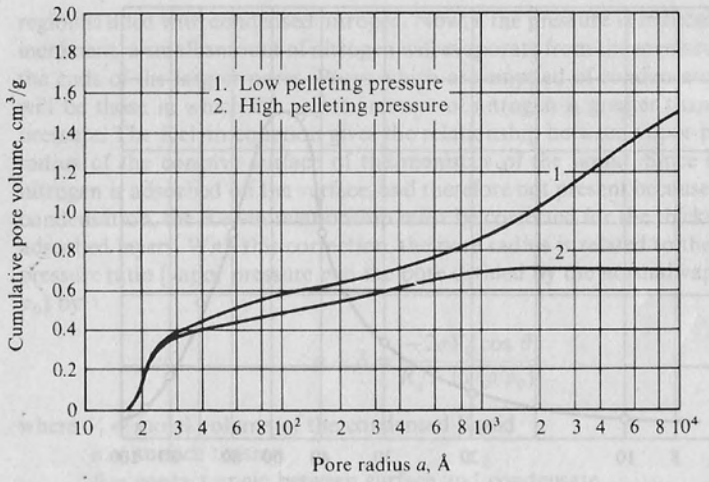

Figure 8-7 Pore volume in alumina (boehmite) pellets.

the surface area. The derivative of the volume curves in Fig. 8-7 gives the pore-volume distribution, and these results are shown in Fig. 8-8. In this figure the bidisperse pore system, characteristic of alumina pellets, is clearly indicated. The micropore range within the particles is narrow, with a most probable radius of 20 Å. The macropores cover a much wider range of radii and show the effect of pelleting pressure. For the high-pressure pellet all volume with pores greater than 2000 Å has been squeezed out, while the most probable radius for the low-pressure pellet is 8000 Å. Pelleting pressure seems to have little effect on the micropores, which suggests that the particles themselves are not crushed significantly during the pelleting process.

Some models (see Chap. 11) for quantitative treatment of the effectiveness of the internal catalyst surface require only the average pore radius $\bar{a}$, rather than the distribution of pore volumes. Wheeler† has developed a simple equation for $\bar{a}$

† A. Wheeler, in P. H. Emmett (ed.), "Catalysis," vol. II, chap. 2, Reinhold Publishing Corporation, New York, 1955.

Table 8-4 Properties of boehmite ($Al_2O_3 \cdot H_2O$) pellets

Pelleting pressure	Macropore volume, cm^3/g	Micropore volume, cm^3/g	Surface area, m^2/g
Low	1.08	0.56	389
High	0.265	0.49	381

Notes: Volume and surface area refer to mass of Al_2O_3 obtained by ignition of boehmite. The pore-volume distribution is given in Fig. 8-8. Average particle size from which pellets were made was 85 microns.

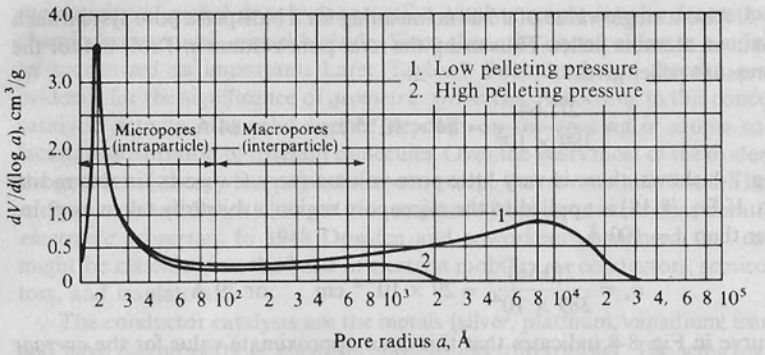

Figure 8-8 Pore-volume distribution in alumina pellets.

which requires only surface-area and pore-volume measurements. Suppose all the pores in a hypothetical particle are straight, cylindrical, not interconnected, and have the same radius $\bar{a}$ and length $\bar{L}$. The average pore radius may be found by writing equations for the total surface and volume in the hypothetical particle and equating these quantities to the surface $m_p S_g$ and volume $m_p V_g$ in the actual particle; i.e.

$$m_p S_g = (2\pi\bar{a}\bar{L})n \tag{8-16}$$

$$m_p V_g = (\pi\bar{a}^2\bar{L})n \tag{8-17}$$

where m_p and n are the mass and number of pores per particle. Dividing the two equations gives the average pore radius,

$$\bar{a} = \frac{2V_g}{S_g} \tag{8-18}$$

This expression agrees well with volume-average values obtained from the distribution curve for monodisperse pore systems. For example, from the data for the Vycor sample (Fig. 8-6) Eq. (8-18) gives

$$\bar{a} = \frac{2(0.208)}{90 \times 10^4} = 46 \times 10^{-8} \text{ cm} \qquad \text{or } 46 \text{ Å}$$

The volume-average value is calculated from the pore volume data used to obtain the distribution curve (Fig. 8-6) and the expression

$$\bar{a} = \frac{\int_0^{V_g} a\, dV}{V_g}$$

By this method $\bar{a} = 45$ Å.

Accurate values of the small areas existing in macropore systems make it difficult to use Eq. (8-18) to calculate $\bar{a}$ for interparticle pores. Hence the average radius for systems such as the UO_2 pellets discussed in Example 8-6 should be obtained by integrating under the cumulative-volume-vs.-$\bar{a}$ curve shown in

Fig. 8-5. Also a single value of $\bar{a}$ has no meaning for a bidisperse pore system such as that in an alumina pellet. Thus using the *total* pore volume in Table 8-4 for the low-pressure pellet gives

$$\bar{a} = \frac{2(1.64)}{389 \times 10^4} = 84 \times 10^{-8} \text{ cm} \qquad \text{or } 84 \text{ Å}$$

As Fig. 8-8 shows, there is very little pore volume (very few pores) in this radius region. If Eq. (8-18) is applied to the micropore region, arbitrarily taken as pores smaller than $a = 100$ Å,

$$\bar{a}_\mu = \frac{2(0.56)}{389 \times 10^4} = 29 \times 10^{-8} \text{ cm} \qquad \text{or } 29 \text{ Å}$$

The curve in Fig. 8-8 indicates that this is an approximate value for the *average* pore radius in the micropore region. Note that the micropore distribution is asymmetrical in such a way that the average radius is greater than the most probable value (20 Å).

Summary In concluding the treatment of physical properties of catalysts, let us review the purpose for studying properties and structure of porous solids. Heterogeneous reactions with solid catalysts occur on parts of the surface active for chemisorption. The number of these active sites and the rate of reaction is, to a first approximation, proportional to the extent of the surface. Hence it is necessary to know the surface area. This is evaluated by low-temperature-adsorption experiments in the pressure range where a monomolecular layer of gas (usually nitrogen) is physically adsorbed on the catalyst surface. The effectiveness of the interior surface of a particle (and essentially all of the surface is in the interior) depends on the volume and size of the void spaces. The pore volume (and porosity) can be obtained by simple pycnometer-type measurements (see Examples 8-4 and 8-5). The average size (pore radius) can be estimated by Eq. (8-18) from the surface area and pore volume in some *monodisperse* systems. Determination of the complete distribution of pore volume according to pore radius requires either mercury-penetration measurements or nitrogen-adsorption data at pressures where capillary condensation occurs, or both. Accurate values of the average pore radius can be evaluated from such pore-volume-vs.-radius data. Note also that a measurement of the complete nitrogen-adsorption-desorption isotherm is sufficient to calculate surface area and pore volume, and distribution of pore sizes, in the range $10 \text{ Å} < a < 200$ Å.

8-4 Theories of Heterogeneous Catalysis

Understanding how solid catalysts work has been an elusive and challenging problem. Several theories have gained prominence, only to lose acceptance as *general* explanations of catalytic activity as additional experimental evidence becomes available. In chronological order, Sabatier† suggested that a mechanism for

† P. Sabatier, "Catalysis in Organic Chemistry," trans. by E. E. Reid, in "Catalysis, Then and Now," Franklin Publishing Company, Englewood, N.J., 1965.

the activity of nickel as a hydrogenation catalyst might involve formation of a chemical compound, nickel hydride. Since then, the *chemical factor* continues to be recognized as important. Later Taylor,* Balandin,† and Beeck‡ provided evidence for the significance of *geometric properties*. According to this concept the catalytic activity of a solid surface depends on the spacing of atoms so as to facilitate adsorption of reactant molecules. Over the years most of the evidence for the geometric theory has proved suspect, except that for metallic films. The work of Boudart§ and Beeck changed the emphasis from geometric considerations to *electronic properties*. In 1948 Dowden and coworkers¶ proposed that catalysts might be classified, on the basis of electron mobility, as conductors, semiconductors, and insulators.

The conductor catalysts are the metals (silver, platinum, vanadium, iron, etc.) and have the property of chemisorption by electron transfer. The semiconductor catalysts are the oxides, such as NiO, Cu_2O, and ZnO. These materials have the capability of interchanging electrons from the filled valence bands in a compound when sufficient energy is provided, for example, by heating. Upon this electron transfer the semiconductor becomes a conductor.†† The insulator catalysts include such widely used substances as silica gel, alumina, and their combinations. Even at high temperatures, electrons are not supposed to be able to move through these two solids freely enough to justify their being called conductors. These substances are also known to be strong acids. Their activity in the many hydrocarbon reactions which they catalyze is presumably due to the formation of carbonium ions at the acid sites on the surface. Carbonium-ion mechanisms are well described in the original work of Whitmore‡‡ and the later work of Greensfelder.§§ It should be emphasized that the electronic theory is not without uncertainties and at present should be considered as a concept in transition.¶¶ However, it does provide a convenient, and probably helpful, method of classifying solid catalysts.

In order fully to understand the behavior of solid catalysts the chemical structure of the adsorbed species must be known. Up to now this has been an

* H. S. Taylor, *Proc. Roy. Soc.* (*London*), **A108**, 105 (1925).

† A. A. Balandin, "Advances in Catalysis," vol. X, p. 96, Academic Press, Inc., New York, 1958.

‡ O. Beeck, *Disc. Faraday Soc.*, **8**, 118 (1950).

§ M. Boudart, *J. Am. Chem. Soc.*, **72**, 1040 (1950).

¶ D. A. Dowden, *Research*, **1**, 239 (1948); D. A. Dowden and P. W. Reynolds, *Disc. Faraday Soc.*, **8**, 187 (1950).

†† Semiconductors are classified as *p* type if they tend to attract electrons from the chemisorbed species, or as *n* type if they donate electrons to this species. The *p* type are normally the compounds, such as NiO. The *n* type are substances which contain small amounts of impurities, or the oxide is present in nonstoichiometric amounts (as, for example, when some of the zinc in ZnO has been reduced). Reviews of semiconductors as catalysts are given by P. H. Emmett ("New Approaches to the Study of Catalysis," 36th Annual Priestly Lectures, Pennsylvania State University, April 9–13, 1962) and by P. G. Ashmore ("Catalysis and Inhibition of Chemical Reactions," Butterworth & Co. (Publishers), London, 1963.

‡‡ F. C. Whitmore, *J. Am. Chem. Soc.*, **54**, 3274 (1932).

§§ B. S. Greensfelder, "Chemistry of Petroleum Hydrocarbons," vol. II, chap. 27, Reinhold Publishing Corporation, New York, 1955.

¶¶ An analysis of the electronic theory is given by Th. Volkenstein, in "Advances in Catalysis," vol. XII, p. 189, Academic Press Inc., New York, 1960.

unsolved problem, except for a few special cases. However, recent progress in developing and improving spectroscopic techniques for examing surface and bulk properties of solids provides encouragement. These techniques include x-ray scattering, nuclear magnetic resonance, Raman spectroscopy, high resolution electron microscopy, extended x-ray absorption, fine structure spectroscopy, and photoacoustic spectroscopy. It seems unlikely that a general theory of catalysis, applicable to a wide variety of reactions, will emerge. Nevertheless, these new instrumental methods may provide explanations for the behavior of many important catalytic processes.

8-5 Classification of Catalysts

From an accumulation of practical experience it is possible to narrow the range of solids that are likely to be catalysts for a type of chemical reaction. We discuss a few cases here and give information for more reactions in Table 8-5.

Metals chemisorb oxygen and hydrogen and therefore are usually effective catalysts for oxidation-reduction and hydrogenation-dehydrogenation reactions. Thus platinum is a successful catalyst for the oxidation of SO_2, and Ni is used effectively for hydrogenation of hydrocarbons. The metals oxides, as semiconductors, catalyze the same kinds of reactions, but often higher temperatures are required. Because of the relative strength of the chemisorption bond with which such gases as O_2 and CO are attached to metals, these gases are poisons when metals are employed as hydrogenation catalysts. The semiconductor oxides are less susceptible to such poisoning. Oxides of the transition metals, such as MoO_3 and Cr_2O_3, are good catalysts for polymerization of olefins. Also aluminum alkyl-titanium chloride [for example, $Al(C_2H_5)_3 + TiCl_4$] constitutes an excellent catalyst for producing isotactic polymers from olefins.† Alumina and silica catalysts are widely used for alkylation, isomerization, polymerization, and particularly for cracking of hydrocarbons. In each case the mechanism presumably involves carbonium ions formed at the acid sites on the catalyst. While the emphasis here has been on solid catalysts, liquid and gaseous acids, particularly H_2SO_4 and HF, are well-known alkylation and isomerization catalysts.

Often catalysts are specific. An important example is the effectiveness of iron for producing hydrocarbons from hydrogen and carbon monoxide (the Fischer-Tropsch synthesis). Dual-function catalysts for isomerization and reforming reactions consist of two active substances in close proximity to each other. For example, Ciapetta and Hunter‡ found that a silica-alumina catalyst upon which nickel was dispersed was much more effective in isomerizing *n*-hexane than silica alumina alone. The explanation depends on the fact that olefins are more readily isomerized than paraffin hydrocarbons. Nickel presumably acts as a dehydrogenating agent, producing hexene, after which the silica alumina isomerizes the hexene to isohexene. Finally, the nickel is effective in hydrogenating hexene back to isohexane.

† K. Ziegler, *Angew. Chem.*, **64**, 323 (1952); G. Natta and I. Pasquon, in "Advances in Catalysis," vol. XI, p. 1, Academic Press Inc., New York, 1959.

‡ F. G. Ciapetta and J. B. Hunter, *Ind. Eng. Chem.*, **45**, 155 (1953).

Table 8-5 Catalysts for Commercial Processes†

Process	Typical catalysts	Poisons
Alkylation of hydrocarbons	$H_2SO_4(l)$, $HF(l)$, $AlCl_3 + HCl$ H_3PO_4/kieselguhr	Substances which reduce acidity
Hydrocarbon cracking	Crystalline synthetic SiO_2-Al_2O_3 (zeolites)	Nitrogen compounds, metals (Ni, V, Cu) coke deposition
Chlorination of hydrocarbons	$CuCl_2/Al_2O_3$	
Dehydration	γ-Al_2O_3, SiO_2-Al_2O_3, WO_3	Coke deposition
Dehydrogenation	Cr_2O_3/Al_2O_3, Fe, Ni, Co, ZnO, Fe_2O_3	H_2O
Desulfurization of petroleum fractions	Sulfided Co-Mo/Al_2O_3	
Fischer-Tropsch process	Ni/kieselguhr, $Fe + Fe_2C + Fe_3O_4$	
Hydrogen from naphtha, coal	Ni/refractory	Sulfur, arsenic, coke deposition
Hydrogenation	Ni/kieselguhr, NiO, Ni-Al (Raney nickel), Pt/Al_2O_3, Pd/Al_2O_3, Ru/Al_2O_3	Sulfur, chlorine compounds
Hydrocracking of coal, heavy oil	NiS, Co_2O_3-MoO_3/Al_2O_3 W_2O_3, $ZnCl_2$	
Isomerization	$AlCl_3 + HCl$, Pt/Al_2O_3	
Oxidation, inorganic	Pt, V_2O_5, Rh, $CuCl_2$(HCl to Cl_2)	Arsenic, chlorine compounds
Oxidation, organic (liquid phase)	$CuCl_2(aq) + PdCl_2$, Pd/Al_2O_3, Co + Cu acetates	
Oxidation, organic (gas phase)	V_2O_5/Al_2O_3, Ag-AgO, CuO bismuth molybdate	
Polymerization	$Al(C_2H_5)_3$, P_2O_5/kieselguhr, MoO_3 -CoO/Al_2O_3, $CrO_3/(SiO_2$-$Al_2O_3)$, $TiCl_3$-$Al(C_2H_5)_3$	H_2O, O_2, sulfur compounds CO, CO_2

† Condensed from material in "Catalytic Processes and Proven Catalysts" by Charles L. Thomas, Academic Press, New York, 1970.

Much has and is being written on solid catalysts, and helpful sources of summary information are available.†‡

8-6 Catalyst Preparation

Experimental methods and techniques for catalyst manufacture are particularly important because chemical composition is not enough by itself to determine activity. The physical properties of surface area, pore size, particle size, and particle structure also have an influence. These properties are determined to a large

† P. H. Emmett (ed.), "Catalysis," Reinhold Publishing Corporation, New York, 1954–; "Advances in Catalysis," Academic Press Inc., New York, 1949–; *J. Catalysis*, **1**, 1962–; A. A. Balandin, "Scientific Selection of Catalysts," trans. by A. Aledjem, Davey Publishing Company, Hartford, Conn., 1968.

‡ J. H. Sinfelt, *AIChE J.*, **19**, 673 (1973).

extent by the preparation procedure. To begin with, a distinction should be drawn between preparations in which the entire material constitues the catalyst and those in which the active ingredient is dispersed on a *support* or *carrier* having a large surface area. The first kind of catalyst is usually made by precipitation, gel formation, or simple mixing of the components.

Precipitation provides a method of obtaining the solid material in a porous form. It consists of adding a precipitating agent to solutions of the desired components. Washing, drying, and usually calcination and activation (or pretreatment) are subsequent steps in the process. For example, a magnesium oxide catalyst can be prepared by precipitating the magnesium from nitrate solution by adding sodium carbonate. The precipitate of $MgCO_3$ is washed, dried, and calcined to obtain the oxide. Such variables as concentration of the aqueous solutions, temperature, and time of the drying and calcining steps may influence the surface area, pore structure, and intrinsic activity of the final product. This illustrates the difficulty in reproducing catalysts and indicates the necessity of carefully following tested recipes. Of particular importance is the washing step to remove all traces of impurities, which may act as poisons.

A special case of the precipitation method is the formation of a colloidal precipitate which gels. The steps in the process are essentially the same as for the usual precipitation procedure. Catalysts containing silica and alumina are especially suitable for preparation by gel formation, since their precipitates are of a colloidal nature. Detailed techniques for producing catalysts through gel formation or ordinary precipitation are given by Ciapetta and Plank.†‡

In some instances a porous material can be obtained by mixing the components with water, milling to the desired grain size, drying, and calcining. Such materials must be ground and sieved to obtain the proper particle size. A mixed magnesium and calcium oxide catalyst can be prepared in this fashion. The carbonates are milled wet in a ball machine, extruded, dried, and reduced by heating in an oven.

Catalyst *carriers* provide a means of obtaining a large surface area with a small amount of active material. This is important when expensive agents such as platinum, palladium, ruthenium, and silver are used.§ Berkman *et al.*¶ have treated the subject of carriers in some detail.

The steps in the preparation of a catalyst impregnated on a carrier may include (1) evacuating the carrier, (2) contacting the carrier with the impregnating solution, (3) removing the excess solution, (4) drying, (5) calcination and activation. For example, a nickel hydrogenation catalyst can be prepared on alumina by soaking the evacuated alumina particles with nickel nitrate solution, draining to remove the excess solution, and heating in an oven to decompose the nitrate to nickel oxide. The final step (activation), reduction of the oxide to metallic nickel, is

† F. G. Ciapetta and C. J. Plank, in P. H. Emmett (ed.), "Catalysis," vol. I, chap. 7, Reinhold Publishing Corporation, New York, 1954.

‡ J. R. Anderson "Structure of Metallic Catalysts", Academic Press, New York, 1975.

§ Such metals are normally deposited only on the outer region of the particle.

¶ S. Berkman, J. C. Morrell, and G. Egloff, "Catalysis," Reinhold Publishing Corporation, New York, 1940.

best carried out with the particles in place in the reactor by passing hydrogen through the equipment. Activation *in situ* prevents contamination with air and other gases which might poison the reactive nickel. In this case no precipitation was required. This is a desirable method of preparation, since thorough impregnation of all the interior surface of the carrier particles is relatively simple. However, if the solution used to soak the carrier contains potential poisons such as chlorides or sulfates, it may be necessary to precipitate the required constituent and wash out the possible poison.

The nature of the support can affect catalyst activity and selectivity. This effect presumably arises because the support can influence the surface structure of the atoms of dispersed catalytic agent. For example, changing from a silica to alumina carrier may change the electronic structure of deposited platinum atoms. This question is related to the optimum amount of catalyst that should be deposited on a carrier. When only a small fraction of a monomolecular layer is added, increases in amount of catalyst should increase the rate. However, it may not be helpful to add large amounts to the carrier. For example, the conversion rate of the ortho to para hydrogen with a NiO catalyst deposited on alumina was found† to be less for 5.0 wt % NiO than for 0.5 wt % NiO. The dispersion of the catalyst on the carrier may also be an important factor in such cases. The nickel atoms were deposited from a much more concentrated $NiNO_3$ solution to make the catalyst containing 5.0 wt % NiO. This may have led to larger clusters of nickel atoms. That is, many more nickel atoms were deposited on top of each other, so that the dispersion of nickel on the surface was less uniform than with the 0.5 wt % catalyst. It is interesting to note that a 5.0 wt % NiO catalyst prepared by 10 individual depositions of 0.5 wt % was much more active (by a factor of 11) than the 5.0 wt % added in a single treatment. The multiple deposition method presumably gave a much larger active nickel surface, because of better dispersion of the nickel atoms on the Al_2O_3 surface. Since the total amount of nickel was the same for the two preparations, one would conclude that the individual particles of nickel were smaller in the 10-application catalyst. These kinds of data indicate the importance of measuring surface areas for chemisorption of the reactants involved. A technique based on the chemisorption of H_2 and CO has been developed‡ to study the effect of dispersion of a catalyst on its activity and the effect of interaction between catalyst and support on activity.

8-7 Promoters and Inhibitors

As normally used, the term "catalyst" designates the composite product used in a reactor. Components of the catalyst include the catalytically active substance itself and may also include a carrier, promoters, and inhibitors.

Innes§ has defined a *promoter* as a substance added during the preparation of

† N. Wakao, J. M. Smith, and P. W. Selwood, *J. Catalysis*, **1**, 62 (1962).

‡ G. K. Boreskov and A. P. Karnaukov, *Zh. Fiz. Khim.*, **26**, 1814 (1952); L. Spenadel and M. Boudart, *J. Phys. Chem.*, **64**, 204 (1960).

§ W. B. Innes, in P. H. Emmett (ed.), "Catalysis," vol. 1, chap. 7, Reinhold Publishing Corporation, New York, 1954.

a catalyst which improves activity or selectivity or stabilizes the catalytic agent so as to prolong its life. The promoter is present in a small amount and by itself has little activity. There are various types, depending on how they act to improve the catalyst. Perhaps the most extensive studies of promoters has been in connection with iron catalysts for the ammonia synthesis reaction.† It was found that adding Al_2O_3 (other promoters are CaO, K_2O) prevented reduction (by sintering) in surface area during catalyst use and gave an increased activity over a longer period of time. Chlorides are sometimes added as promoters to hydrogenation and isomerization catalysts, and sulfiding improves hydro-desulfurization (Co-Mo) catalysts. Some promoters are also believed to increase the number of active centers and so make the existing catalyst surface more active. The published information on promoters is largely in the patent literature.

An *inhibitor* is the opposite of a promoter. When added in small amounts during catalyst manufacture, it lessens activity, stability, or selectivity. Inhibitors are useful for reducing the activity of a catalyst for an undesirable side reaction. For example, silver supported on alumina is an excellent oxidation catalyst. In particular, it is used widely in the production of ethylene oxide from ethylene. However, at the same conditions complete oxidation to carbon dioxide and water also occurs, so that selectivity to C_2H_4O is poor. It has been found that adding halogen compounds to the catalyst inhibits the complete oxidation and results in satisfactory selectivity.

8-8 Catalyst Deactivation (Poisoning)

The activity of a catalyst normally decreases with time. In the development of a new catalytic process, the life of the catalyst is usually a major economic consideration. Shutting down a process, and its associated separation and preparation units, for regenerating or replacing catalyst is prohibitive except at infrequent intervals. In many instances, very active catalytic substances have been discovered only to be discarded because activity cannot be maintained and regeneration was not practical. Hence, an understanding of how catalysts lose activity is important. In some systems the catalyst activity decreases so slowly that exchange for new material, or regeneration, is required only at intervals measured in months or years. Examples are promoted catalysts for synthetic ammonia and catalysts containing metals such as platinum and silver. Catalysts for cracking and some other hydrocarbon reactions, however, lose much of their activity in seconds. The decrease in activity is due to *poisons*, which will be defined here as substances, either in the reactants stream or produced by the reaction, which lower the activity of the catalyst. The continuous (or frequent) regeneration of cracking catalysts is necessary because of the deposition of one of the products, carbon, on the surface.

The slow decrease is usually due to chemisorption of reactants, products, or impurities in the liquid stream. Rapid deactivation is caused by physically depositing a substance which blocks the active sites of the catalyst. We will use the term *poisoning* to describe both processes, although rapid deactivation is also called

† P. H. Emmett and S. Brunauer, *J. Am. Chem. Soc.*, **62**, 1732 (1940).

fouling. Deactivation can also be caused by a change in the surface structure of the catalyst (e.g., sintering) due to prolonged exposure to elevated temperature in the reacting atmosphere. In this section we list and briefly describe poisons. Quantitative treatment and the effect of deactivation on intrinsic rates of catalytic reactions are considered in Sec. 9-6. The effect on the global rate, which includes the influence of intraparticle diffusion, is taken up in Sec. 11-14.

Poisons can be differentiated in terms of the way in which they operate. Many summaries listing specific poisons and fouling reactions are available.† The following arrangement has been taken in part from Innes.

Deposited poisons Carbon deposition on catalysts used in the petroleum industry falls into this category. The carbon covers the active sites of the catalyst and may also partially plug the pore entrances. This type of poisoning is at least partially reversible, and regeneration can be accomplished by burning to CO and CO_2 with air and/or steam. The regeneration process itself is a heterogeneous reaction, a gas-solid noncatalytic one. In the design of the reactor, attention must be given to the regeneration as well as to the reaction parts of the cycle.‡

Chemisorbed poisons Compounds of sulfur and other materials are frequently chemisorbed on nickel, copper, and platinum catalysts. The decline in activity stops when equilibrium is reached between the poison in the reactant stream and that on the catalyst surface. If the strength of the adsorption bond is not great, the activity will be regained when the poison is removed from the reactants. If the adsorbed material is tightly held, the poisoning is more permanent. The mechanism appears to be one of covering the active sites, which could otherwise adsorb reactant molecules.

Selectivity poisons The selectivity of a solid surface for catalyzing one reaction with respect to another is not well understood. However, it is known that some materials in the reactant stream will adsorb on the surface and then catalyze other undesirable reactions, thus lowering the selectivity. The very small quantities of nickel, vanadium, iron, etc., in petroleum stocks may act as poisons in this way. When such stocks are cracked, the metals deposit on the catalyst and act as dehydrogenation catalysts. This results in increased yields of hydrogen and coke and lower yields of gasoline.

Stability poisons When water vapor is present in the sulfur dioxide–air mixture supplied to a platinum-alumina catalyst, a decrease in oxidation activity occurs. This type of poisoning is due to the effect of water on the structure of the alumina

† R. H. Griffith, "The Mechanism of Contact Catalysis," p. 93, Oxford University Press, New York, 1936; E. B. Maxted, *J. Soc. Chem. Ind. (London)*, **67**, 93 (1948); P. H. Emmett (ed.), "Catalysis," vol. 1, chap. 6, Reinhold Publishing Corporation, New York, 1954. An extensive review by J. B. Butt, Chemical Reaction Engineering, Adv. Chemistry Series, **109**, 259 (1972); B. W. Wojciechowski, *Catal. Rev.* **9**, 79 (1974).

‡ Typical references are M. Sagara, S. Masamune, and J. M. Smith, *AIChE J.*, **13**, 1226 (1967); G. F. Froment and K. B. Bischoff, *Chem. Eng. Sci.*, **16**, 189 (1961); P. B. Weisz and R. D. Goodwin, *J. Catalysis*, **2**, 397 (1963).

Table 8-6 Poisons for various catalysts

Catalyst	Reaction	Types of poisoning	Poisons
Silica, alumina	Cracking	Chemisorption	Organic bases
		Deposition	Carbon
		Stability	Water
		Selectivity	Heavy metals
Nickel, platinum, copper	Hydrogenation Dehydrogenation	Chemisorption	Compounds of S, Se, Te, P, As, Zn, halides, Hg, Pb, NH_3, C_2H_2, H_2S, Fe_2O_3, etc.
Cobalt	Hydrocracking	Chemisorption	NH_3, S, Se, Te, P
Silver	$C_2H_4 + O \rightarrow C_2H_4O$	Selectivity	CH_4, C_2H_6
Vanadium oxide	Oxidation	Chemisorption	As
Iron	Ammonia synthesis	Chemisorption	O_2, H_2O, CO, S, C_2H_2
	Hydrogenation	Chemisorption	Bi, Se, Te, P, H_2O
	Oxidation	Chemisorption	VSO_4, Bi

Source: In part from W. B. Innes in P. H. Emmett (ed), "Catalysis," vol. I, chap. 7, p. 306, Reinhold Publishing Corporation, New York, 1954.

carrier. Temperature has a pronounced effect on stability poisoning. Sintering and localized melting may occur as the temperature is increased, and this, of course, changes the catalyst structure.

Diffusion poisons This kind of poisoning has already been mentioned in connection with carbon deposition on cracking catalysts. Blocking the pore mouths prevents the reactants from diffusing into the inner surface. Entrained solids in the reactants, or fluids which can react with the catalyst to form a solid residue, can cause this type of poisoning.

Tables 8-5 and 8-6 list poisons for various catalysts and reactions. The materials that are added to reactant streams to improve the performance of a catalyst are called *accelerators*. They are the counterparts of poisons. For example, steam added to the butene feed of a dehydrogenation reactor appeared to reduce the amount of coke formed and increase the yield of butadiene. The catalyst in this case was iron.†

PROBLEMS

8-1 The silica gel for *n*-hexane adsorption mentioned in Prob. 7-6 has the following properties: $S_g = 832\ m^2/g$, $\varepsilon_p = 0.486$, $\rho_p = 1.13\ g/cm^3$, $V_g = 0.43\ cm^3/g$. Using the adsorption data given in Prob. 7-6: (*a*) Estimate the fraction of the surface covered with an adsorbed monomolecular layer at each partial pressure of *n*-hexane. The surface occupied by one molecule of hexane at 70°C is estimated to be $58.5 \times 10^{-16}\ cm^2$; (*b*) Calculate the value of $\bar{C}_m$ from the total surface area and the area occupied by one molecule of hexane. What conclusions can be drawn from the comparison of this value of $\bar{C}_m$ with that obtained in Prob. 7-6?

† K. K. Kearly, *Ind. Eng. Chem.*, **42**, 295 (1950).

8-2 Repeat Prob. 8-1 for benzene adsorption on the same silica gel but at 110°C. The surface occupied by one benzene molecule is estimated to be $34.8 \times 10^{-16}\ cm^2$. Use the adsorption data for benzene given in Prob. 7-7.

8-3 Refer to Prob. 7-12. Using a constant value of $34.8 \times 10^{-16}\ cm^2$ for the surface area occupied by one molecule of benzene, determine the fractional surface coverage at each partial pressure of benzene given in Prob. 7-12.

8-4 Curve 3 of Fig. 8-2 is a Brunauer-Emmett-Teller plot for the adsorption data of N_2 at −183°C on the sample of silica gel. The density of liquid N_2 at this temperature is $0.751\ g/cm^3$. Estimate the area of the silica gel from these data, in square meters per gram, and compare with the results of Example 8-2.

8-5 The "point-*B* method" of estimating surface areas was frequently used prior to the development of the Brunauer-Emmett-Teller approach. It entailed choosing from an adsorption diagram such as Fig. 8-1 the point at which the central linear section begins. This procedure worked well for some systems, but it was extremely difficult, if not impossible, to select a reliable point *B* on an isotherm such as that shown for *n*-butane in Fig. 8-1. In contrast, the Brunauer-Emmett-Teller method was found to be reasonably satisfactory for this type of isotherm. Demonstrate this by estimating the surface area of the silica gel sample from the *n*-butane curve in Fig. 8-1 (multiply the ordinate of the *n*-butane curve by 10). The density of liquid butane at 0°C is $0.601\ g/cm^3$.

8-6 An 8.01-g sample of Glaucosil is studied with N_2 adsorption at −195.8°C. The following data are obtained:

Pressure, mmHg	6	25	140	230	285	320	430	505
Volume adsorbed, cm^3 (at 0°C and 1 atm)	61	127	170	197	215	230	277	335

The vapor pressure of N_2 at −195.8°C is 1 atm. Estimate the surface area (square meters per gram) of the sample.

8-7 Low-temperature (−195.8°C) nitrogen-adsorption data were obtained for an Fe-Al_2O_3 ammonia catalyst. The results for a 50.4-g sample were:

Pressure, mmHg	8	30	50	102	130	148	233	258	330	442	480	507	550
Volume adsorbed, cm^3 (at 0°C and 1 atm)	103	116	130	148	159	163	188	198	221	270	294	316	365

Estimate the surface area for this catalyst.

8-8 Ritter and Drake† give the true density of the solid material in an activated alumina particle as $3.675\ g/cm^3$. The density of the particle determined by mercury displacement is 1.547. The surface area by adsorption measurement is $175\ m^2/g$. From this information compute the pore volume per gram, the porosity of the particles, and the mean pore radius. The bulk density of a bed of the alumina particles in a $250\text{-}cm^3$ graduate is $0.81\ g/cm^3$. What fraction of the total volume of the bed is void space between the particles and what fraction is void space within the particles?

8-9 Two samples of silica-alumina cracking catalysts have particle densities of 1.126 and $0.962\ g/cm^3$, respectively, as determined by mercury displacement. The true density of the solid material in each case

† H. L. Ritter and L. C. Drake, *Ind. Eng. Chem., Anal. Ed.*, **17**, 787 (1945).

is 2.37 g/cm^3. The surface area of the first sample is 467 m^2/g and that of the second is 372 m^2/g. Which sample has the larger mean pore radius?

8-10 Mercury porosimeter data are tabulated below for a 0.400-g sample of UO_2 pellet. At the beginning of the measurements ($p = 1.77$ lb/in.^{2} abs) the mercury displaced by the sample was 0.125 cm^3. At this low pressure no pores were penetrated. Data obtained with a pycnometer gave a true density of the solid phase of $\rho_S = 7.57$ g/cm^3.

Calculate the total porosity of the pellet and the porosity due to pores of larger than 250 Å radius. Also plot the pore-volume distribution for the pores larger than 250 Å radius, using the coordinates of Fig. 8-5.

Pressure, lb/in.^{2}	196	296	396	500	600	700	800	900
Mercury penetration, cm^3	0.002	0.004	0.008	0.014	0.020	0.026	0.032	0.038

	1000	1200	1400	1800	2400	2800	3400	5000
	0.044	0.052	0.057	0.062	0.066	0.066	0.067	0.068

CHAPTER

NINE

RATE EQUATIONS FOR FLUID-SOLID CATALYTIC REACTIONS

The nonuniformity of catalyst surfaces and lack of accurate knowledge of the structure of chemisorbed species and their concentrations have been emphasized in Chaps. 7 and 8. In view of these uncertainties it is debatable how much detail should be postulated in formulating equations for rates of reaction. The most simple approach, wholly empirical, would be to use the power-law form of the rate equation, employed for homogeneous reactions, that is, Eq. (2-9). The values of the exponents on the concentrations, the apparent orders of the reaction, are determined by fitting the equation to the data. This approach ignores all the problems associated with adsorption and catalytic surfaces and provides no information about how the reaction occurs. Frequently, but not always, such an equation can correlate experimental rates just as accurately, and with fewer adjustable parameters, than more elaborate methods. When the objective is reactor design, where calculations of engineering accuracy are going to be made with the rate equation, the simplicity of the power-law form is advantageous. Hence, it has been used widely in industrial reactor design. As examples, such equations have been used to represent kinetics data for the water-gas shift reaction using iron oxide catalysts†

$$CO + H_2O \rightleftarrows H_2 + CO_2$$

and for the methanation reaction

$$CO_2 + 4H_2 \rightleftarrows CH_4 + 2H_2O$$

on a Ru/Al_2O_3 catalyst.‡

† H. Bohlbro, "An Investigation on the Kinetics of the Conversion of Carbon Monoxide with Water Vapor Over Iron Oxide Catalysts", 2d ed. Gjellerup, Copenhagen, 1969.

‡ P. J. Lunde and F. L. Kester, *J. Catal.*, **30**, 423 (1973).